ELSEVIER

A Heitler model of extensive air showers

J. Matthews *

Department of Physics and Astronomy, Louisiana State University, Baton Rouge, LA 70803, USA
Department of Physics, Southern University, Baton Rouge, LA 70813, USA

Abstract

A simple, semi-empirical model is used to develop the hadronic portion of air showers in a manner analogous to the well-known Heitler splitting approximation of electromagnetic cascades. Various characteristics of EAS are plainly exhibited with numerical predictions in good accord with detailed Monte Carlo simulations and with data. Results for energy reconstruction, muon and electron sizes, the elongation rate, and for the effects of the atomic number of the primary are discussed.
© 2004 Elsevier B.V. All rights reserved.

1. Introduction

Extensive air showers develop in a complex way as a combination of electromagnetic cascades and hadronic multiparticle production. It is necessary to perform detailed numerical simulations of air showers to infer the properties of the primary cosmic rays that initiate them. But simulations are a challenge since the number of charged particles in a high energy shower can be enormous, perhaps exceeding 10^{10}. The design of algorithms is also

hampered by limited knowledge of interaction cross-sections and particle production at high energies.

Before the era of high-speed computing, Heitler presented a very simple model of electromagnetic (EM) cascade development [1]. He and others in that time (notably Rossi [2]) also developed more sophisticated analytical tools, which included more physical effects. Such approaches, past and present, are well described by Gaisser [3].

We will consider here Heitler's simplest conception of EM cascades and extend it to the case of extensive air showers. The purpose of using a very simple model is to show plainly the physics involved. It cannot replace fully detailed

---

* Address: Department of Physics and Astronomy, Louisiana State University, Baton Rouge, LA 70803, USA.
E-mail address: matthews@phys.lsu.edu

simulations. Nevertheless, Heitler's EM model predicted accurately the most important features of electromagnetic showers.

Heitler's model (Fig. 1a) has e^+, e^-, and photons undergoing repeated two-body splittings, either one-photon bremsstrahlung or e^+e^- pair production. Every particle undergoes a splitting after it travels a fixed distance related to the radiation length. After n splittings there are 2^n total particles in the shower. Multiplication abruptly ceases when the individual $e^\pm$ energies drop below the *critical energy* ξ_c^e, where average collisional energy losses begin to exceed radiative losses.

This simplified picture does not capture accurately all details of EM showers. But two very important features are well accounted for: the final total number of electrons, positrons, and photons N_{max} is simply proportional to $E_\circ$ and the depth of maximum shower development is logarithmically proportional to $E_\circ$.

We approximate hadronic interactions similarly [4]. For example, Fig. 1b shows a proton striking an air molecule, and a number of pions emerging from the collision. Neutral pions decay to photons almost immediately, producing electromagnetic subshowers. The $\pi^\pm$ travel some fixed distance and interact, producing a new generation of pions.

The multiplication continues until individual pion energies drop below a critical energy ξ_c^π, where it begins to become more likely that a $\pi^\pm$ will decay rather than interact. All $\pi^\pm$ are then as-sumed to decay to muons which are observed at the ground.

This first approximation assumes that interactions are perfectly inelastic, with all the energy going into production of new pions. We will study the more realistic case which includes a leading particle carrying away a significant portion of the energy later (Section 4).

The important difference between a hadronic cascade and a pure EM shower is that a third of the energy is "lost" from new particle production at each stage from π° decay. Thus the total energy of the initiating particle is divided into two channels, hadronic and electromagnetic. The primary energy is linearly proportional to a combination of the numbers of EM particles and muons.

We examine the model in detail below. In particular, we will look at its predictions for measurable properties of extensive air showers, attempting to assess which predictions are reliable and which may not be. First, we review the specifics of Heitler's electromagnetic shower model and then develop the hadronic analogue. In all that follows, the term "electron" does not distinguish between e^+ and e^-.

2. Electromagnetic showers

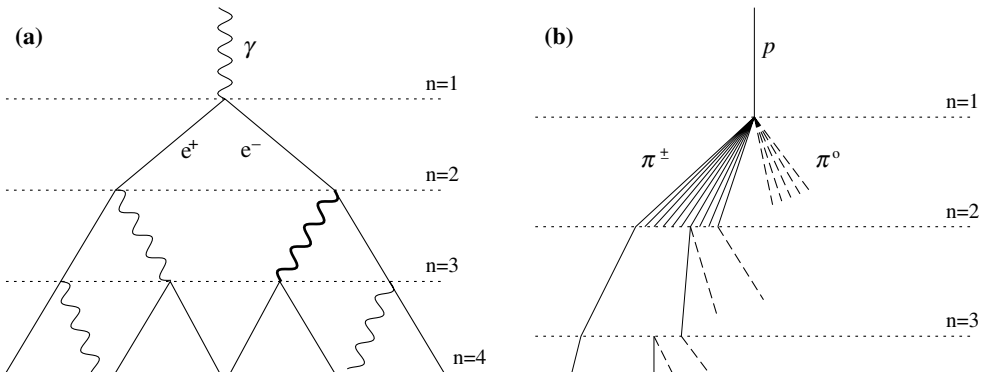As seen in Fig. 1a, an electron radiates a single photon after traveling one *splitting length*

Fig. 1. Schematic views of (a) an electromagnetic cascade and (b) a hadronic shower. In the hadron shower, dashed lines indicate neutral pions which do not re-interact, but quickly decay, yielding electromagnetic subshowers (not shown). Not all pion lines are shown after the $n = 2$ level. Neither diagram is to scale.

$d = \lambda_r \ln 2$, where λ_r is the radiation length in the medium. (Note that d is in fact the distance over which an electron loses, on average, half its energy by radiation.) After traveling the same distance, a photon splits into an e^+e^- pair. In either instance, the energy of a particle (electron or photon) is assumed to be equally divided between two outgoing particles. After n splitting lengths, a distance of $x = n\lambda_r \ln 2$, the total shower size (electrons and photons) is $N = 2^n = e^{x/\lambda_r}$.

Multiplication ceases when the energies of the particles are too low for pair production or bremsstrahlung. Heitler takes this energy to be the critical energy ξ_c^e, below which radiative energy loss becomes less than collisional energy loss. In air, $\xi_c^e = 85$ MeV.

Consider a shower initiated by a single photon with energy $E_\circ$. The cascade reaches maximum size $N = N_{max}$ when all particles have energy ξ_c^e, so that

$$E_\circ = \xi_c^e N_{max}. \tag{1}$$

The penetration depth X_{max} at which the shower reaches maximum size is obtained by determining the number n_c of splitting lengths required for the energy per particle to be reduced to ξ_c^e. Since $N_{max} = 2^{n_c}$, we obtain from Eq. (1) that $n_c = \ln[E_\circ/\xi_c^e]/\ln 2$, giving

$$X_{max}^\gamma = n_c \lambda_r \ln 2 = \lambda_r \ln[E_\circ/\xi_c^e]. \tag{2}$$

The superscript "γ" emphasizes that this expression is appropriate for purely electromagnetic showers; the case for an air shower with hadronic components is considered later. The *elongation rate* Λ is the rate of increase of X_{max} with $E_\circ$, defined as

$$\Lambda \equiv \frac{dX_{max}}{d\log_{10}E_\circ}, \tag{3}$$

so that using X_{max} from Eq. (2) yields $\Lambda^\gamma = 2.3\lambda_r = 85$ g cm^{-2} per decade of primary energy for EM showers in air.

Fig. 2 shows a detailed EGS4 simulation [5] of an electromagnetic cascade in iron ($\lambda_r = 13.8$ g cm^{-2}, $\xi_c^e = 22.4$ MeV). Heitler's model predicts a maximum total size $N_{max} = 1340$, about a factor of two larger than the sum of electrons and photons in the figure. It can be seen that the shower has begun to attenuate before reaching
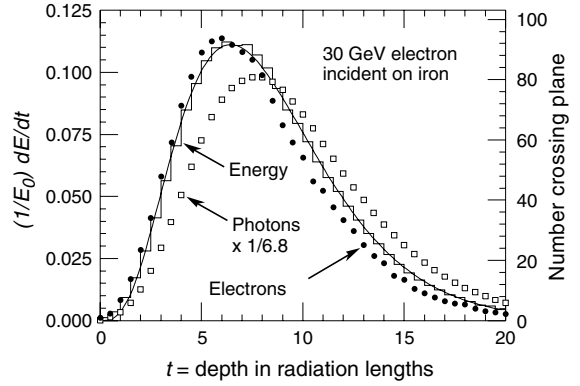

Fig. 2. EGS4 simulation of electromagnetic showering in iron. Points are particles or photons, the curve shows energy deposition in each layer.

maximum. The model does not treat the loss of particles as they range out. Also note that this simulation does not display particles below 1.5 MeV. We conclude that the Heitler model predicts the shower size fairly well, if it is interpreted carefully. The predicted depth of maximum from Eq. (2) is $7.4\lambda_r$, is in very good accord with the full simulation.

Note that the final EM size N_{max} predicted by the model may differ significantly from what is actually *measured* by an experiment. The attenuation of particle numbers is not accounted for in the model, and in commonly used detectors such as scintillators, $e^\pm$ give much stronger signals than photons do. It is useful therefore to differentiate $e^\pm$ and photons in the previous expressions.

The model overestimates the actual ratio of electrons to photons (as was noted by Heitler [1]). It predicts that after a few generations, the electron size approaches $N_e \approx \frac{2}{3}N_{max}$. This is much too large for several reasons, mainly that multiple photons are often radiated during bremsstrahlung. Moreover, many $e^\pm$ range out in the air. Such details of the development of the shower near and beyond its maximum are beyond the scope of this model, requiring careful treatment of particle production and energy loss.

Simulations confirm that photons greatly outnumber electrons throughout the development of the shower, as seen in Fig. 2. At their respective maxima, the number of photons is more than a

factor of six larger than the number of $e^\pm$. The maximum electron size is an order of magnitude less than Heitler's predicted N_{max}. These ratios hold true in other media and at much higher energies as well, with nearly identical values found in simulations of 10^{14} eV γ-rays in air [6] and in PeV proton air showers (described in the next section).

To extract the number of electrons N_e from Heitler's overall size N, we will simply adopt a correction factor:

$$N_e = N/g, \tag{4}$$

with a constant value of $g = 10$. This should be considered an order of magnitude estimate. Further adjustments can be made to g when comparing the model to actual experimental measurements.

Despite its limitations, the Heitler model reproduces two basic features of EM shower development which are confirmed by detailed simulations and by experiments:

- The maximum size of the shower is proportional $E_\circ$,
- The depth of maximum increases logarithmically with energy, at a rate of 85 gcm^{-2} per decade of primary energy.

3. Hadronic showers

Air showers initiated by hadrons (Fig. 1b) are modeled using an approach similar to Heitler's. The atmosphere is imagined in layers of fixed thickness $\lambda_I \ln 2$, where λ_I is now the *interaction length* of strongly interacting particles. λ_I is assumed to be constant, a fairly good approximation for interactions in the range 10–1000 GeV. For pions in air, $\lambda_I \approx 120$ gcm^{-2} [3].

Hadrons interact after traversing one layer, producing N_{ch} charged pions and $\frac{1}{2}N_{ch}$ neutral pions. A π° immediately decays to photons, initiating electromagnetic showers. Charged pions continue through another layer and interact. The process continues until the $\pi^\pm$ fall below the critical energy ξ_c^π where they then are all assumed to decay, yielding muons.

We first develop the model for air showers initiated by cosmic ray protons. These results will then be extended to include heavier nuclei as the primaries.

3.1. Model parameters

Following Heitler's EM shower approach, we attempt to keep parameters as constants, as far as possible. For the sake of concreteness, we will consider numerical factors appropriate for a range of energies bracketing the "knee" region of the primary spectrum, $E_\circ = 10^{14}$ eV to 10^{17} eV.

We also will use the same electron reduction factor $g = 10$ (as in Eq. (4)) to estimate the fraction of the particle size which is actually observed. Detailed simulations and experiments show that the ratio of photons to electrons in an air shower is very similar to that seen in a purely EM cascade. Fig. 3 shows this ratio at ground level, from a full simulation [7] of proton induced extensive air showers ($E_\circ = 1$ PeV), as a function of the photon or electron energy at the ground. Very similar results have been obtained elsewhere for showers initiated by 10^{15} eV gamma rays [6].

The multiplicity N_{ch} of charged particles produced in hadron interactions increases very slowly with laboratory energy, growing as $E^{1/5}$ in pp and
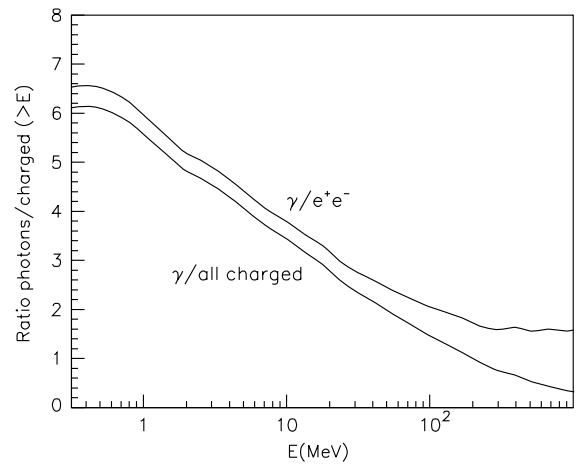

Fig. 3. Ratio of photons to electrons, and photons to all charged particles, at ground level from a simulated proton induced, 1 PeV extensive air shower. E is the photon or electron energy at the ground.

$p\bar{p}$ data [8]. Since the multiplicity in π-nucleon collisions is similar [10], we adopt a constant value $N_{ch} = 10$, a value accurate to within a factor of two for pion kinetic energies from about 1 GeV through 10 TeV. But we will remain cautious of the validity of this approximation. The great majority of interactions in a shower occur with pion energies of order 100 GeV, much lower than the primary energy $E_\circ$. However, there are circumstances—study of X_{max} for example—where the properties of the *first* interaction have more importance.

The other important parameter in our model is ξ_c^π, the energy at which we assume that further particle production by $\pi^\pm$ ceases. We estimate ξ_c^π as the energy at which the decay length of a charged pion becomes less than the distance to the next interaction point.

Consider a single cosmic ray proton entering the atmosphere with energy $E_\circ$. After n interactions (or atmospheric layers) there are $N_\pi = (N_{ch})^n$ total charged pions. Assuming equal division of energy during particle production, these pions carry a total energy of $(2/3)^n E_\circ$. The remainder of the primary energy $E_\circ$ has gone into electromagnetic showers from π° decays. The energy per charged pion in atmospheric layer n is therefore

$$E_\pi = \frac{E_\circ}{\left(\frac{3}{2}N_{ch}\right)^n}. \tag{5}$$

After a certain number n_c of generations, E_π becomes less than ξ_c^π.

For example, in a shower initiated by a 10^{15} eV primary proton, individual pion energies after four interactions are $E_\pi = 10^{15}/\left(\frac{3}{2}10\right)^4 = 20$ GeV, using $N_{ch} = 10$. The decay length of a pion with this energy is $\gamma c\tau = 1.1$ km. Assuming an exponential atmospheric density profile with scale height 8 km, the linear distance between the altitudes of the beginning and the end of the fourth interaction layer is 1.8 km. This is the first layer that pions have encountered where their probability of a decay exceeds that of arriving at the next interaction point. The critical energy in this shower is then $\xi_c^\pi = 20$ GeV.

If we repeat the above exercise at other primary energies, we find that $\xi_c^\pi = 30$ GeV at $E_\circ = 10^{14}$ eV and $\xi_c^\pi = 10$ GeV at $E_\circ = 10^{17}$ eV. It is evident that

ξ_c^π slowly decreases with increasing primary energy. Hereafter we adopt a constant value $\xi_c^\pi = 20$ GeV.

The number of interactions needed to reach $E_\pi = \xi_c^\pi$ is, from Eq. (5),

$$n_c = \frac{\ln[E_\circ/\xi_c^\pi]}{\ln\left[\frac{3}{2}N_{ch}\right]} = 0.85\log_{10}[E_\circ/\xi_c^\pi], \tag{6}$$

giving $n_c = 3, 4, 5, 6$ for $E_\circ = 10^{14}, 10^{15}, 10^{16}, 10^{17}$ eV respectively. Eq. (6) does not depend strongly on moderate variations of the value chosen for N_{ch}. For example, using $N_{ch} = 20$ changes n_c only above $E_\circ = 10^{16}$ eV, reducing it by one.

As a last check of the self-consistency of our choices for N_{ch} and ξ_c^π, we look at the properties of the interactions in the cascade. In the above examples, the average kinetic energy of all the interacting pions in a shower is about 250 GeV, nearly independently of $E_\circ$. This energy corresponds to $\sqrt{s} = 22$ GeV for pions colliding with stationary nucleons. The mean pp charged multiplicity at this energy is about 8 [5]. Allowing for multiple interactions of a pion colliding with a target air nuclei, our selection of $N_{ch} = 10$ seems quite reasonable.

In the following sections we implement the hadronic shower model adopting the following (constant) values for the parameters: $N_{ch} = 10$, $\xi_c^e = 85$ MeV, $\xi_c^\pi = 20$ GeV, $\lambda_I = 120$ g/cm^2, $\lambda_r = 37$ g/cm^2.

3.2. Primary energy

The primary energy is finally divided between N_π pions and N_{max} electromagnetic particles in subshowers. The number of muons is $N_\mu = N_\pi$. By analogy to Eq. (1), the total energy in this case is

$$E_\circ = \xi_c^e N_{max} + \xi_c^\pi N_\mu.$$

Scaling to the electron size $N_e = N_{max}/g$ as before,

$$E_\circ = g\xi_c^e\left(N_e + \frac{\xi_c^\pi}{g\xi_c^e}N_\mu\right)$$
$$\approx 0.85 \text{ GeV } (N_e + 24N_\mu). \tag{7}$$

Eq. (7) represents energy conservation. The relative magnitude of the contributions from N_μ and

from N_e is determined by their respective critical energies—the energy scales at which electromagnetic and hadronic multiplication cease. Different primaries allocate energy differently between the electromagnetic and hadronic components, as do statistical fluctuations. Eq. (7) implicitly accounts for these differences.

The importance of the result in Eq. (7) is that $E_\circ$ is simply calculable if both N_e and N_μ are measured. The relation is linear and insensitive both to fluctuations and to primary particle type.

The practical use of Eq. (7) requires adjustments to account for experimental details. One effect is that measurements of particles are usually made after shower maximum. Another is that the relative sensitivity of an experiment to photons and electrons affects the interpretation of measured value of N_e.

Fig. 4 shows the energy reconstruction published by the CASA-MIA group [11]. Their result has $E_\circ = 0.8$ GeV $(N_e + 25N_\mu)$, where N_e and N_μ are measured shower sizes. Note that the relation is linear and independent of the primary particle type. In light of the caveats above, it must be considered somewhat accidental that the numerical coefficients in their result agree so precisely with Eq. (7).
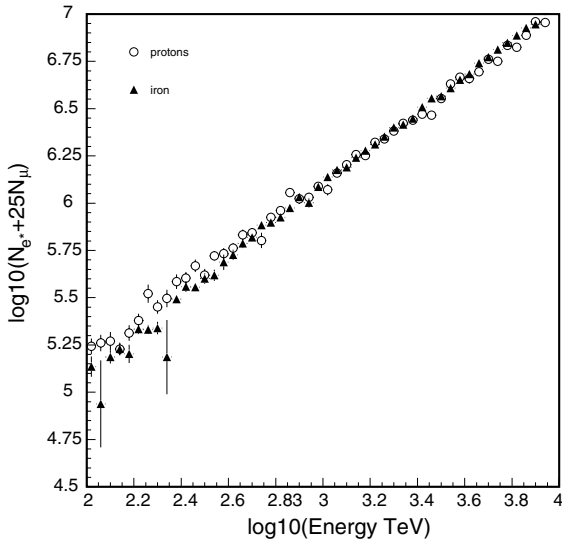

Fig. 4. Energy reconstruction from CASA-MIA (from [11]).

3.3. Muon and electron sizes

The number of muons in the shower is obtained using $N_\mu = N_\pi = (N_{ch})^{n_c}$. The energy dependence of the muon size is obtained by using Eq. (6) to cast N_μ in the form

$$\ln N_\mu = \ln N_\pi = n_c \ln N_{ch} = \beta \ln[E_\circ / \xi_c^\pi],$$

where

$$\beta = \frac{\ln[N_{ch}]}{\ln\left[\frac{3}{2}N_{ch}\right]} = 0.85. \tag{8}$$

Note that although N_{ch} in fact changes as the shower develops, β depends only logarithmically on its value. If N_{ch} were an order of magnitude larger, $\beta = 0.92$. So our assumption that N_{ch} is constant has little impact. The muon size of the shower is then

$$N_\mu = \left(\frac{E_\circ}{\xi_c^\pi}\right)^\beta \approx 10^4 \left(\frac{E_\circ}{1\text{ PeV}}\right)^{0.85}. \tag{9}$$

Recent studies using several detailed Monte Carlo simulations report values $\beta = 0.85 \to 0.92$ [9,10]. Our present model will match these values very well when we include the effects of leading particles in hadron interactions (see Section 4). In any case, the less-than-linear growth of N_μ with primary energy has important consequences for modeling showers initiated by nuclei heavier than protons, described later.

We estimate the electron size of the shower by assessing how much energy has gone into electromagnetic channels, assume it appears as EM subshowers, and then use Eq. (1) to obtain N. This approximation simply adds all the EM subshowers from each interaction generation to determine the total number of electrons produced.

Conservation of energy implies that the primary energy is split into electromagnetic and hadronic parts $E_\circ = E_{em} + E_h$. The hadronic energy appears in the muon component as $E_h = N_\mu \xi_c^\pi$, so that the fraction into the EM component is

$$\frac{E_{em}}{E_\circ} = \frac{E_\circ - N_\mu \xi_c^\pi}{E_\circ} = 1 - \left(\frac{E_\circ}{\xi_c^\pi}\right)^{\beta-1}, \tag{10}$$

where β is from Eq. (9). The EM fraction is 72% at $E_\circ = 10^{14}$ eV, rising to 90% at $E_\circ = 10^{17}$ eV. Eq.

(10) can be well approximated by a power law $E_{em} \propto E_\circ^\alpha$ in the energy region of interest here. After comparing series expansions near $E_\circ = 10^5 \xi_c^\pi$, we obtain

$$N_e = \frac{1}{g} \frac{E_{em}}{\xi_c^e} \approx 10^6 \left(\frac{E_\circ}{1\ \text{PeV}} \right)^\alpha,$$

where

$$\alpha = 1 + \frac{1-\beta}{10^{5(1-\beta)} - 1} \approx 1.03.$$

Inverting this expression gives

$$E_\circ = (1.5\ \text{GeV}) N_e^{0.97}, \tag{11}$$

in good agreement with full simulations of Engel et al. [9], which gave $E_\circ = (1.6\ \text{GeV}) N_e^{0.99}$. It should be emphasized that N_e in Eq. (16) is to be interpreted as the electron size at shower maximum.

3.4. Depth of shower maximum

X_{max} is the atmospheric depth at which the electrons and photons of the air shower reach their maximum numbers. The EM component is generated by photons from π° decays. The first interaction diverts $\frac{1}{3} E_\circ$ into these channels. This is followed by additional showers from each subsequent interaction point.

We will use only the first generation γ showers to estimate the depth where the shower reaches maximum size. The method previously employed to calculate N_e (Eq. (16)) is inappropriate here. In that case we summed all the electromagnetic energy and treated it as a single EM shower. For proper evaluation of X_{max}, it would be necessary to sum each generation of subshowers carefully from their respective points of origin, accounting for their attenuation near and after their maxima. As we have noted, such treatment is beyond the scope of the simple model we are using.

Using only the first interaction will certainly underestimate X_{max}, since it neglects the following subshowers, but it will capture well the elongation rate Λ^p (the rate of increase of X_{max} with $E_\circ$).

We shall take extra care here to account for the energy dependence both of the primary interaction cross-section and of the multiplicity of produced particles in the first interaction. Each tends to raise the estimated altitude of shower maximum when compared to our previous method which used constant parameters. The interaction cross-section rises with energy, causing air showers to begin higher. The multiplicity of produced pions also increases, giving individual π° lower energy and hence the EM subshowers from their decays will have shorter development lengths.

The first interaction occurs at an atmospheric depth $X_\circ = \lambda_I \ln 2$, where λ_I is in this case the interaction length of the primary *proton*. Using the inelastic p-air cross-section from [10], we approximate λ_I to obtain

$$X_\circ = \lambda_I \ln 2$$
$$= (61\ \text{g cm}^{-2})(1.0 - 0.1 \ln[E_\circ/\text{PeV}]) \ln 2.$$

The first interaction yields $\frac{1}{2} N_{ch} \pi^\circ \rightarrow N_{ch}$ photons. Each photon initiates an electromagnetic shower of energy $E_\circ/(3N_{ch})$, developing in parallel with the others. We parameterise the charged particle production in the *first* interaction as $N_{ch} = 41.2(E_\circ/1\ \text{PeV})^{1/5}$, based on *pp* data [8].

The depth of maximum is now obtained as in Eq. (2), for an EM shower of energy $E_\circ/(3N_{ch})$ starting at depth $X_\circ$, and using the energy-dependencies of $X_\circ$ and N_{ch}:

$$X_{max}^p = X_\circ + \lambda_r \ln \left[E_\circ/(3N_{ch}\xi_c^e) \right]$$
$$= (470 + 58\log_{10}[E_\circ/1\ \text{PeV}])\ \text{g cm}^{-2}. \tag{12}$$

As we expected, these values of X_{max}^p are low when compared to detailed simulations [12,13], by about $100\ \text{g cm}^{-2}$ or a bit less than $2\lambda_I$. Presumably this is the consequence of neglecting the contributions of the next one or two generations of π° production. Also, including the effects of leading particle production (Section 4 below), systematically raises X_{max}^p by about $17\ \text{g cm}^{-2}$.

Fig. 5 shows the model predictions alongside the simulation results. The solid lines are adapted from simulations [12,13] using several modern interaction generators (QGSJET, SIBYLL, neXus, DPMJET). Dashed lines are proton and iron showers from the model. The dotted line represents the photon induced EM showers. Note that both the proton and the iron lines have been shifted upward by $100\ \text{g cm}^{-2}$ to more closely
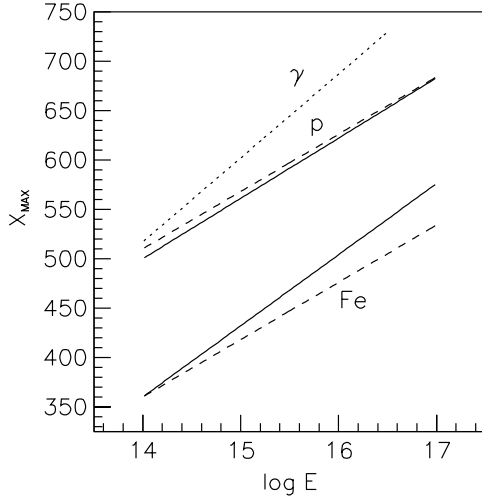
Fig. 5. Depth of maximum vs. primary energy for air showers. Dotted: photon induced showers; Dashed: proton and iron induced showers, each uniformly shifted higher by $100 \, \mathrm{g \, cm^{-2}}$. Solid lines are from full simulations of p and Fe showers.

match the others at 10^{14} eV, but the curve for EM showers is taken directly from Eq. (2). The constant separation between the iron and proton lines is what the model predicts, as will described in the next section.

The predicted elongation rate $\Lambda^{\mathrm{p}} = 58 \, \mathrm{g \, cm^{-2}}$ per decade of energy is in excellent accord with simulations [10].

It is instructive to compare proton induced air showers to purely electromagnetic cascades by rewriting Eq. (12) as

$$X_{\max}^{\mathrm{p}} = X_{\max}^{\gamma} + X_{\circ} - \lambda_{\mathrm{r}} \ln[3N_{\mathrm{ch}}],$$

where $X_{\max}^{\gamma}$ is the depth of maximum of EM showers from Eq. (2). The elongation rate for proton showers is then

$$\Lambda^{\mathrm{p}} = \Lambda^{\gamma} + \frac{\mathrm{d}}{\mathrm{d} \log_{10} E_{\circ}} \{X_{\circ} - \lambda_{\mathrm{r}} \ln[3N_{\mathrm{ch}}]\}$$
$$= 58 \, \mathrm{g \, cm^{-2}} \text{ per decade},$$

as in Eq. (12). It is now easy to see that Λ^{p} is reduced from Λ^{γ} for EM showers by two effects: increasing multiplicity N_{ch} and increasing cross-section (decreasing $X_{\circ}$). The multiplicity and cross-section reductions are respectively $17 \, \mathrm{g \, cm^{-2}}$ and $10 \, \mathrm{g \, cm^{-2}}$ from $\Lambda^{\gamma} = 85 \, \mathrm{g \, cm^{-2}}$ per decade of

energy. (This illustrates Linsley's *elongation rate theorem* [14], which pointed out that Λ^{γ} for electromagnetic showers represents an upper limit to the elongation rate for hadron showers.)

3.5. Nuclear primaries

The *superposition model* is a simplified view of the interaction of a cosmic ray nucleus with the atmosphere. A nucleus with atomic number A and total energy $E_{\circ}$ is taken to be A individual single nucleons, each with energy $E_{\circ}/A$, and each acting independently. We treat the resulting air shower as the sum of A separate proton air showers all starting at the same point.

We can produce observable shower features by substituting the lower primary energy into the various expressions derived previously for proton showers and summing A such showers where appropriate. The resulting nuclear-initiated shower properties are easily expressed in terms of the corresponding quantities of a proton shower with the same total energy $E_{\circ}$:

$$N_{\mu}^{A} = N_{\mu}^{\mathrm{p}} A^{0.15}, \tag{13}$$

$$X_{\max}^{A} = X_{\max}^{\mathrm{p}} - \lambda_{\mathrm{r}} \ln A, \tag{14}$$

$$E_{\circ} = 0.85 \, \mathrm{GeV} \, (N_{\mathrm{e}} + 25 N_{\mu}). \tag{15}$$

One consequence is that nuclear showers have more muons than proton showers, at the same total primary energy. This results from the less-than-linear growth of the muon number with energy. The lower energy nucleons which initiate the shower generate fewer interaction generations, and so lose less energy to electromagnetic components. An iron shower will have $(56)^{0.15} = 1.8$ times as many muons as a proton shower of the same energy.

The showers from lower energy primaries also do not penetrate as deeply. $X_{\max}$ of iron showers is higher than proton showers by $\lambda_{\mathrm{r}} \ln(56) = 150 \, \mathrm{g \, cm^{-2}}$ at all energies. This is in good accord with simulations [13], as was seen in Fig. 5.

As discussed earlier, the energy assignment (Eq. (15) or Eq. (7)) is unaffected by A because the expression intrinsically accounts for all of the primary energy being distributed into a hadronic

channel (seen as muons) and into electromagnetic showers.

4. Inelasticity

The simple model has neglected one aspect of hadronic interactions which has observable consequences. When two hadrons interact, a significant fraction of the total energy is carried away by a single "leading" particle. This energy is unavailable immediately for new particle production. Treatment of this effect is best done by detailed simulations. Nevertheless, we will try here to include it approximately in our model to understand the effects qualitatively.

The *inelasticity* of a single interaction is described by a parameter κ, defined as the fraction of the total energy directed into new pion production (both $\pi^{\pm}$ and π°). The value of κ has a value of perhaps 0.5, but is not well known at high energy. Neglecting leading particle effects (as we have done so far) corresponds to $\kappa = 1.0$.

Our estimation of the elongation rate is not affected by $\kappa < 1$, since the energy dependence of the multiplicity and cross-sections do not depend on κ. Our energy reconstruction formula (Eq. (7)) is also robust against altering the division of energy between hadronic and electromagnetic components.

We expect that including inelasticity will alter the depth of maximum. If a significant fraction of energy is taken away by a single leading particle then it is unavailable for the first EM subshowers. For example, if $\kappa = 0.5$, then Eq. (12) suggests that $X_{\max}^{p}$ will be higher by approximately $58\log_{10}[2] = 17 \text{ g cm}^{-2}$.

We also expect that the total muon production in a shower will increase more quickly with $E_{\circ}$ than in our simple model, since less energy is "lost" to the electromagnetic channel in each interaction.

In Appendix A, we develop our model in the same fashion as before, but adjusting the method to account for $\kappa < 1.0$. We find that, once again, the muon size increases with energy as

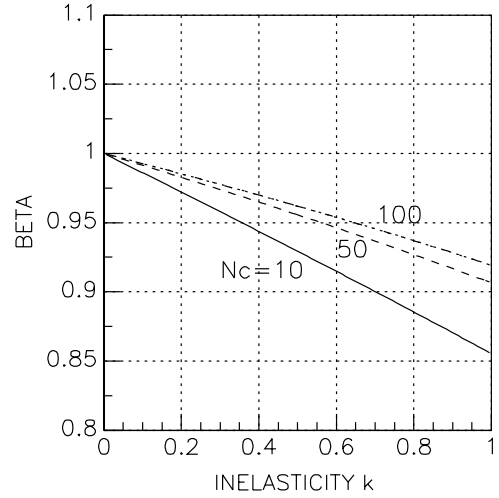$$N_{\mu} = \left(\frac{E_{\circ}}{\xi_{c}^{\pi}}\right)^{\beta},$$

Fig. 6. Variation of muon production index β, from Eq. (16), as a function of inelasticity and charged particle multiplicity N_{ch}.

except now the index is

$$\beta = \frac{\ln[1 + N_{\text{ch}}]}{\ln\left[(1 + N_{\text{ch}})/\left(1 - \frac{1}{3}\kappa\right)\right]}$$
$$\approx 1 - \frac{\kappa}{3\ln[N_{\text{ch}}]} = 1 - 0.14\kappa. \tag{16}$$

The previous relation (Eq. (8)) is simply regained by substituting $(N_{\text{ch}} + 1) \rightarrow N_{\text{ch}}$ and $\kappa = 1$ in the above expression.

For inelasticity $\kappa = 0.5$, the muon size increases at a faster rate ($\beta = 0.93$) than in the original model ($\beta = 0.85$). The effect of inelasticity on the growth of muon size with $E_{\circ}$ is not large, but it is comparable to the effect of assuming a larger average multiplicity N_{ch}. Fig. 6 exhibits Eq. (16), showing the nearly linear dependence of β with κ, for several assumed values of N_{ch}. The resulting expectation that $\beta \simeq 0.90$–0.95 is in better accord with full simulation results [10].

5. Summary

A basic model of extensive air showers, similar to Heitler's model of electromagnetic cascades, gives several predictions which are in good agreement with detailed simulations and with data.

The primary energy is proportional to a combination of the muon and electron sizes,

$E_\circ \sim (N_e + 25N_\mu)$. The relative weighting depends mainly on the characteristic energy scales at which hadronic cascading and electromagnetic showering cease.

Muon size grows with primary energy more slowly than proportionally, $N_\mu \sim E_\circ^\beta$, with $\beta = 0.85$. The exponent depends on the fraction of energy given to charged pions in each interaction. If the model is extended to include significant inelasticity in pion interactions, then $\beta = 0.90$–0.95.

The elongation rate for hadronically induced air showers is $58 \, \mathrm{g\,cm^{-2}}$, less than that from purely electromagnetic showers ($85 \, \mathrm{g\,cm^{-2}}$). The difference arises from the increase of multiplicity with energy in hadronic interactions and on the growth of the p-air inelastic cross-section.

Showers initiated by nuclei with atomic number A will have the same relationship between $E_\circ$ and their muon and electron sizes that protons do. Their depth of maximum will be higher than proton showers by $\lambda_r \ln A$ but the elongation rate is quite similar. The muon size from from nuclear showers will be larger than that from proton showers by a factor of $A^{0.15}$.

Acknowledgments

Appendix A. Inelasticity

When two hadrons interact, a significant fraction of the total energy is carried away by a single leading particle. This energy is unavailable for immediate new particle production. The *inelasticity* can be described by a parameter κ, which we define as the fraction of the total energy directed into pion production.

In an interaction initiated by a particle with energy E, the energy is apportioned as follows:

$(1 - \kappa)E$ is taken by a single leading particle, $\frac{2}{3}\kappa E$ is used to produce N_{ch} charged pions, and $\frac{1}{3}\kappa E$ is carried by $\frac{1}{2}N_{ch}$ neutral pions, subsequently appearing in electromagnetic subshowers.

We will assume that inelasticity effects will be present in all hadron interactions and that κ is constant throughout. We will also assume that in each interaction the total multiplicity of produced charged particles is $(1 + N_{ch})$. This is higher than in the model described before (by one particle), but this formulation is useful for making comparisons. Our simple model is recovered by taking the limit $\kappa \to 1$, and only counting particles with non-zero energy.

The fraction of the energy of an interaction which goes to particles which may interact again (i.e, all except π°) is $(1 - \frac{1}{3}\kappa)$. As before, these particles travel a distance $\lambda_I \ln 2$ and then interact, producing more particles. In a cascade initiated by a primary with energy $E_\circ$, the total energy carried by interacting hadrons after n interactions (or atmospheric layers) is $(1 - \frac{1}{3}\kappa)^n E_\circ$, distributed over $(1 + N_{ch})^n$ charged pions.

However, unlike the simple cascade model, this energy is not evenly distributed among all the hadrons, but instead is carried by groupings of particles whose energies are determined by the value of κ. It is useful to consider the hadronic energy in layer n by explicitly separating the part due to the leading particle $(1 - \kappa)$ from the inelastic, pion-producing component $(\frac{2}{3}\kappa)$:

$$\left(1 - \frac{1}{3}\kappa\right)^n = \left((1 - \kappa) + \frac{2}{3}\kappa\right)^n$$
$$= \sum_{r=0}^n C_{n,r}(1 - \kappa)^{n-r}\left(\frac{2}{3}\kappa\right)^r, \qquad (A.1)$$

where $C_{n,r}$ is the binomial coefficient $\binom{n}{r} = n!/(n-r)!r!$. The number of particles produced which contribute to hadron production in an interaction can be similarly expressed in terms of one leading particle and N_{ch} charged pions. Then, in layer n, the number of such particles is

$$(1 + N_{ch})^n = \sum_{r=0}^n C_{n,r}N_{ch}^{n-r}. \qquad (A.2)$$

The terms in Eq. (A.1) and Eq. (A.2) correspond to one another, as can be seen by (tedious) count-

Table A.1
Properties of the particle groups in the $n = 4$ layer of a cascade. The last two columns give specific numbers for the case where the primary energy is $E_\circ = 10^{15}$ eV, $N_{ch} = 10$, and $\kappa = 0.5$

Pion group r	Number in group	Total energy in group	Number ($N_{ch} = 10$)	Energy per pion ($\kappa = 0.5$)
0	1	$(1 - \kappa)^4 E_\circ$	1	63 TeV
1	$4N_{ch}$	$4(2/3\kappa)(1 - \kappa)^3 E_\circ$	40	4.2 TeV
2	$6N_{ch}^2$	$6(2/3\kappa)^2(1 - \kappa)^2 E_\circ$	600	280 GeV
3	$4N_{ch}^3$	$4(2/3\kappa)^3(1 - \kappa)E_\circ$	4000	19 GeV
4	N_{ch}^4	$(2/3\kappa)^4 E_\circ$	10,000	1.2 GeV

ing as the cascade develops. In interaction generation n, it turns out that there are $n + 1$ separate groups of pions with common energies. For example, in layer $n = 4$, there are five distinct groupings of particles. The properties of the groups are given in Table A.1.

There are more particles in this cascade than in the simple model, beyond what would be expected from simply incrementing N_{ch} by one. For example, when $E_\circ = 1$ PeV, there are almost 50% more particles in the $n = 4$ layer of this cascade. But most (>95%) of the particles are in the two groups with the lowest energy per pion. So we are not too far wrong if we proceed as before, and approximate the terminal interaction layer n_c as the layer where the *average* energy per pion is the critical energy:

$$\xi_c^\pi = \frac{E_\circ \left(1 - \frac{1}{3}\kappa\right)^{n_c}}{\left(1 + N_{ch}\right)^{n_c}},$$

which implies

$$n_c = \frac{\ln[E_\circ/\xi_c^\pi]}{\ln\left[(1 + N_{ch})/\left(1 - \frac{1}{3}\kappa\right)\right]}.$$

This is the same as Eq. (6) with the substitutions $\frac{3}{2} \rightarrow (1 - \kappa/3)^{-1}$ and $N_{ch} \rightarrow (1 + N_{ch})$. As before, we obtain the relation between muon number and primary energy by following the method leading to Eq. (9):

$$\ln N_\mu = \ln N_\pi = n_c \ln[1 + N_{ch}] = \beta \ln[E_\circ/\xi_c^\pi],$$

so that

$$N_\mu = \left(\frac{E_\circ}{\xi_c^\pi}\right)^\beta$$

with

$$\beta = \frac{\ln[1 + N_{ch}]}{\ln\left[(1 + N_{ch})/\left(1 - \frac{1}{3}\kappa\right)\right]}$$

$$\approx 1 - \frac{\kappa}{3\ln[N_{ch}]} = 1 - 0.14\kappa. \tag{A.3}$$

References

[1] W. Heitler, The Quantum Theory of Radiation, third ed., Oxford University Press, London, 1954, p. 386 (Section 38).
[2] B. Rossi, High Energy Particles, Prentice-Hall, Englewood Cliffs, NJ, 1952.
[3] T.K. Gaisser, Cosmic Rays and Particle Physics, Cambridge University Press, Cambridge, 1990.
[4] J. Matthews, in: Proc. 27th ICRC, Hamburg, 2001, p. 261.
[5] Particle Data Group, Review of particle physics, Phys. Rev. D 66 (2002) 203, Fig. 26-17.
[6] N.N. Kalmykov, et al., in: Proc. 28th ICRC, Tsukuba, vol. 2, 2003, p. 511.
[7] S.J. Sciutto, in: Proc. 27th ICRC, Hamburg, 2001, p. 237.
[8] Particle Data Group, Review of particle physics, Phys. Rev. D 66 (2002) 258, Fig. 39-5.
[9] R. Engel, et al., in: Proc. 26th ICRC, vol. 1, Salt Lake City, 1999, p. 415.
[10] J. Alvarez-Muñiz, et al., Phys. Rev. D 66 (2002) 033011.
[11] M.A.K. Glasmacher, et al., Astropart. Phys. 12 (2000) 1–17.
[12] D. Heck, et al., in: Proc. 27th ICRC, Hamburg, 2001, p. 233.
[13] J.W. Fowler, et al., Astropart. Phys. 15 (2001) 49–64.
[14] J. Linsley, in: Proc. 15th ICRC, vol. 12, Plovdiv, 1977, p. 89.
[15] M.A.K. Glasmacher, Ph.D. thesis (unpublished), Univ. of Michigan, 1998.